Meteoritics & Planetary Science 40, Nr 3, 343–360 (2005)
Abstract available online at http://meteoritics.org

Northwest Africa 011: A "eucritic" basalt from a non-eucrite parent body

Christine FLOSS[1*], Larry A. TAYLOR[2], Prinya PROMPRATED[2], and Douglas RUMBLE III[3]

[1]Laboratory for Space Sciences, Washington University, One Brookings Drive, Saint Louis, Missouri 63130, USA
[2]Planetary Geosciences Institute, University of Tennessee, Knoxville, Tennessee 37996, USA
[3]Geophysical Laboratory, Carnegie Institution, Washington, D. C. 20015, USA
[*]Corresponding author. E-mail: floss@wustl.edu

(Received 02 July 2004; revision accepted 17 January 2005)

Abstract–We have carried out a detailed petrographic, mineralogical, and trace element study of Northwest Africa (NWA) 011. This meteorite bears many similarities to the eucrites it was initially identified with, although oxygen isotopic compositions rule out a genetic relationship. Like many eucrites, NWA 011 crystallized from a source with approximately chondritic proportions of REE, although a slightly LREE-enriched bulk composition with a small positive Eu anomaly, as well as highly fractionated Fe/Mg ratios and depleted Sc abundances (Korotchantseva et al. 2003), suggest that the NWA 011 source experienced some pyroxene and/or olivine fractionation. Thermal metamorphism resulted in homogenization of REE abundances within grains, but NWA 011 did not experience the intergrain REE redistribution seen in some highly metamorphosed eucrites. Despite a similarity in oxygen isotopic compositions, NWA 011 does not represent a basaltic partial melt from the acapulcoite/lodranite parent body. The material from which NWA 011 originated may have been like some CH or CB chondrites, members of the CR chondrite clan, which are all related through oxygen isotopic compositions. The NWA 011 parent body is probably of asteroidal origin, possibly the basaltic asteroid 1459 Magnya.

INTRODUCTION

Melting and differentiation of asteroids was a common process in the early solar system, as attested to by the variety of magmatic iron meteorite types (e.g., Scott 1979). However, few of the corresponding silicate differentiates that must have formed on these planetesimals are represented in our meteorite collection. Among the basaltic achondrites, only the eucrites are reasonably abundant and have, with some degree of confidence, been associated with a specific parent body, the asteroid 4 Vesta (McCord et al. 1970; Binzel and Xu 1993). Northwest Africa (NWA) 011 was originally classified as a non-cumulate eucrite (Afanasiev et al. 2000). However, the oxygen isotopic composition of NWA 011 was determined to be very different from that of the eucrites and other known basaltic achondrites (Yamaguchi et al. 2002). In addition, the Fe/Mn values in NWA 011 pyroxene are significantly higher than the values typically associated with eucrites (Afanasiev et al. 2000). Thus, NWA 011 appears to have originated on a distinct parent body and as such has the potential to provide us with fresh insights into asteroidal differentiation processes in the early solar system.

We have carried out a detailed petrographic, mineralogical and trace element investigation of NWA 011 in order to provide additional constraints on the nature of this parent body. Our data show that, while NWA 011 is very similar to eucrites, there are also differences, including evidence for formation under more oxidizing conditions than those experienced by eucrites. Preliminary results of our work have been reported by Promprated et al. (2003) and Floss et al. (2004).

EXPERIMENTAL

We studied the petrography and mineralogy of a thin section of NWA 011 with a total area of 1.7 cm^2. Major element compositions were determined using the fully automated Cameca SX-50 electron microprobe at the University of Tennessee, operated at an accelerating voltage of 15kV, with a 20 nA beam current and counting times of 20 sec. Beam sizes varied depending on the phase being analyzed: a 10 μm beam was used for plagioclase analyses to avoid volatilization of Na, and 5 μm and 1 μm beam sizes were used for pyroxene and olivine and for opaque minerals, respectively. Data were corrected for matrix effects using standard PAP procedures. Prior to trace element analysis, the

Table 1. Mineralogical modes for NWA 011 (vol%).

	1[a]	2[b]	3[c]	Average
Pyroxene (pigeonite + augite)	54.6	58.5	55.3	56.1 ± 2.1
Plagioclase	43.8	39.6	42.2	41.9 ± 2.1
Olivine	0.2	tr	0.1	0.2 ± 0.1
Silica	n.d.	0.7	1.5	1.1 ± 0.6
Phosphate	1.1	0.5	0.4	0.7 ± 0.4
Opaque minerals	0.2	0.7	0.4	0.4 ± 0.3
Total area	1.7 cm^2	2.9 cm^2	0.98 cm^2	

[a]This work.
[b]Promprated et al. (2003).
[c]Yamaguchi et al. (personal communication).
tr = trace; n.d. = not determined.

section was further characterized using the JEOL 840a scanning electron microscope (SEM) at Washington University. X-ray mapping for ten elements (Al, Ca, Cr, Fe, Mg, Na, P, S, Si, Ti) was done of the entire section and custom software, written in LabVIEW, was used to identify phases and calculate the modal composition of the section (mode 1 in Table 1). The resolution of the X-ray maps (256 × 256 pixels at a magnification of 75×; 1 pixel = ~5 μm) did not allow pigeonite and augite to be distinguished. We also did not specifically search for silica; this phase may in fact be present in our section, but is not included in the mode. The major source of uncertainty in the modal determination is likely to be due to the difficulty of determining exact phase boundaries, given the limited resolution of the X-ray maps. However, it is difficult to assign a quantitative error to the mode based on this uncertainty.

Concentrations of the REE and other trace elements were determined using the modified Cameca IMS 3f ion microprobe at Washington University according to techniques described by Zinner and Crozaz (1986a). All analyses were made using an O^- primary beam and energy filtering at low mass resolution to remove complex molecular interferences. The resulting mass spectrum is deconvolved in the mass ranges K-Ca-Sc-Ti, Rb-Sr-Y-Zr, and Ba-REE to remove simple molecular interferences that are not eliminated with energy filtering (Alexander 1994; Hsu 1995). Sensitivity factors for the REE in pyroxene and Ca-phosphate are from Zinner and Crozaz (1986b) and for plagioclase are from Floss and Jolliff (1998). Sensitivity factors for other elements in plagioclase and pyroxene are from Hsu (1995) and are listed in Table 1 of Floss et al. (1998). Absolute concentrations are determined using sensitivity factors relative to Si for the silicates and Ca for the phosphates. The CaO concentrations used for the phosphates (merrillite) are the average of lunar merrillites from Jolliff et al. (1993). SiO_2 concentrations for plagioclase are the average of the values determined by electron microprobe. Pyroxene in NWA 011 is pigeonite containing abundant augite exsolution lamellae. We obtained electron microprobe analyses of the augite lamellae as well as the host pigeonite. Because the ion probe beam was larger than the width of the lamellae, we used an average of the augite and pigeonite concentrations as the reference SiO_2 concentration for the pyroxene analyses. REE abundances in the figures are normalized to the CI abundances of Anders and Grevesse (1989).

Oxygen isotopic analyses were carried out at the Geophysical Laboratory, Carnegie Institution on two separate portions of NWA 011 using a high-precision laser-fluorination technique (Wiechert et al. 2001). Samples weighing 1–2 mg were loaded into a Sharp-type reaction chamber (Sharp 1990), evacuated, pre-fluorinated, and heated with a CO_2 laser in a 25 torr atmosphere of purified BrF_5. The primary $\delta^{18}O$ standard was UWG-2 garnet (Valley et al. 1995). Two secondary standards were also analyzed to bracket the $\delta^{18}O$ of NWA 011. The $\Delta^{17}O$ offset of NWA 011 from the terrestrial fractionation line was determined according to the procedures of Miller (2002).

RESULTS

NWA 011 is a 40 g stone (Grossman 2000) that appears to be a monolithic unbrecciated achondrite consisting mainly of pigeonite and plagioclase with minor amounts of olivine, silica, phosphate, and the opaque minerals, ulvöspinel and ilmenite (Fig. 1). Pigeonite is commonly subhedral and often has curved boundaries at the contacts with plagioclase. Grains range in size from 0.2 to 0.8 mm and contain exsolution lamellae of augite that are typically a few microns wide, but can reach up to ~10 μm in width. Plagioclase grains are anhedral, up to 0.1 mm in size, and usually form crystal aggregates (up to 2 mm across) or straddle along grain boundaries of pigeonite grains (Fig. 1a). This texture probably indicates recrystallization, possibly as a result of thermal metamorphism. However, we did not observe relict plagioclase or augite grains, such as those noted by Yamaguchi et al. (2002). Opaque minerals occur as small clusters, usually together with olivine, and include ulvöspinel, ilmenite, and small FeNi metal-sulfide intergrowths (Fig. 1b). The Ca-phosphates, merrillite and apatite, are common, but are not evenly distributed.

Modal abundances are given in Table 1, where they are compared with others from the literature. Mode 2 was

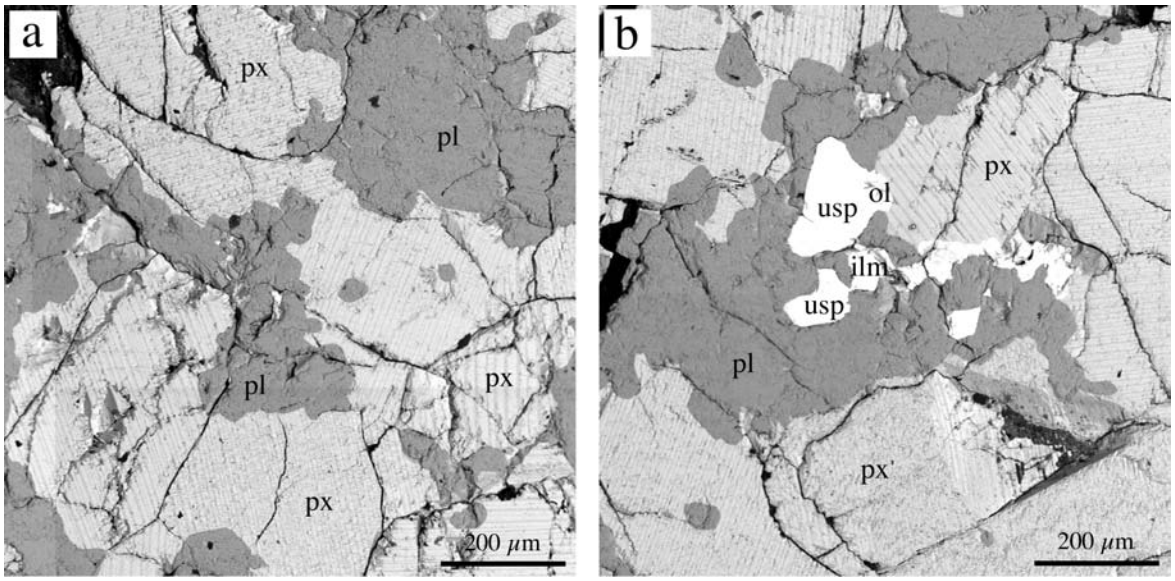

Fig. 1. Backscattered electron (BSE) images of NWA 011: a) subhedral pigeonite with augite exsolution lamellae (px) and anhedral plagioclase (pl) crystal aggregates; b) opaque mineral cluster with ulvöspinel (usp), ilmenite (ilm) and olivine (ol).

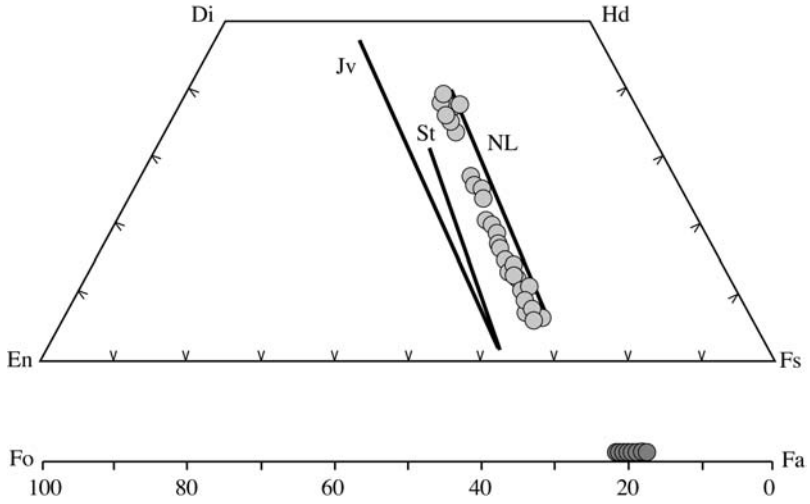

Fig. 2. Major element compositions of pyroxene and olivine from NWA 011. The solid lines in the pyroxene quadrilateral show the compositions of pyroxenes from the Nuevo Laredo trend (NL), Stannnern trend (St), and main group (Juvinas; Jv) eucrites. Data from BVSP (1981) and Warren and Jerde (1987).

reported by Promprated et al. (2003) and was determined by Korochantseva et al. (2003) on a different thin section of NWA 011. Mode 3 was determined by A. Yamaguchi on a third thin section of NWA 011. An average mode, based on all three determinations, is also given in Table 1. There are moderate variations in the relative abundances of plagioclase and pyroxene between the three sections, which probably to a large degree reflect the uncertainties associated with the modal determinations. The accessory phases also appear to be heterogeneously distributed, as has been noted by others (e.g., Yamaguchi et al. 2002).

Mineral compositions are summarized in Table 2. Compositions of pigeonite ($Wo_{5.7–6.5}Fs_{63.2–65.1}$) and the augite lamellae ($Wo_{36.1–39.2}Fs_{35.2–38.3}$) are similar to those of Nuevo Laredo trend eucrites (Fig. 2; Warren and Jerde 1987). However, as has been noted (e.g., Afanasiev et al. 2000), the Fe/Mn ratios are significantly higher than those of typical eucrites (Fig. 3). The plagioclase in NWA 011 is bytownite in composition with low K_2O contents ($An_{80.2–87.7}Or_{0.7–0.2}$). The olivine is Fe-rich and has little variation in composition ($Fa_{79.5–81.4}$; Fig. 2). The compositions of ulvöspinel and ilmenite are given in Table 2. Phosphate compositions were not analyzed by electron microprobe, but EDS spectra taken of the grains analyzed by ion microprobe show that all are merrillite, rather than apatite.

Results of the oxygen isotopic analyses are shown in

Table 2. Major element concentrations (in wt%) in NWA 011 minerals.

	Plagioclase	Pigeonite	Augite lamellae	Olivine	Ilmenite	Ulvöspinel
SiO_2	46.45 ± 0.63	47.79 ± 0.37	48.55 ± 0.40	30.86 ± 0.31	0.16 ± 0.18	0.06 ± 0.02
TiO_2	n.m.	0.52 ± 0.07	0.84 ± 0.11	0.34 ± 0.32	52.72 ± 0.72	24.19 ± 0.31
Cr_2O_3	n.m.	0.18 ± 0.03	0.39 ± 0.07	n.m.	0.10 ± 0.04	13.73 ± 0.41
Al_2O_3	33.42 ± 0.43	0.50 ± 0.04	1.27 ± 0.10	0.03 ± 0.03	0.11 ± 0.14	4.41 ± 0.20
V_2O_3	n.m.	n.m.	n.m.	n.m.	0.26 ± 0.04	0.43 ± 0.05
FeO	0.76 ± 0.70	36.11 ± 0.34	20.41 ± 0.54	59.60 ± 0.34	45.12 ± 0.58	53.27 ± 0.76
MnO	n.m.	0.55 ± 0.03	0.33 ± 0.03	0.55 ± 0.03	0.37 ± 0.01	0.30 ± 0.03
NiO	n.m.	n.m.	n.m.	0.01 ± 0.04	n.m.	n.m.
MgO	0.05 ± 0.09	9.68 ± 0.23	8.51 ± 0.26	8.09 ± 0.31	0.66 ± 0.07	0.51 ± 0.02
CaO	17.21 ± 0.42	2.79 ± 0.10	17.55 ± 0.48	0.20 ± 0.05	0.18 ± 0.10	0.07 ± 0.03
Na_2O	1.62 ± 0.22	0.02 ± 0.01	0.09 ± 0.01	n.m.	n.m.	n.m.
K_2O	0.07 ± 0.02	n.m.	n.m.	n.m.	n.m.	n.m.
P_2O_5	n.m.	n.m.	n.m.	n.m.	n.m.	n.m.
Fe_2O_3[a]	b.d.	1.24	1.11	b.d.	b.d.	2.29
Total	99.58	99.37	99.05	99.67	99.66	99.26
# analyses	16	16	12	9	3	5
	$An_{82.2–87.7}Or_{0.7–0.2}$	$Wo_{5.7–6.5}Fs_{63.2–65.1}$	$Wo_{36.1–39.2}Fs_{35.2–38.3}$	$Fa_{79.5–81.4}$		
Fe/Mn		67	65	108		

[a]Calculated after the method of Spear (1995).
n.m. = not measured; b.d. = below detection. Errors represent the standard deviation from the mean.

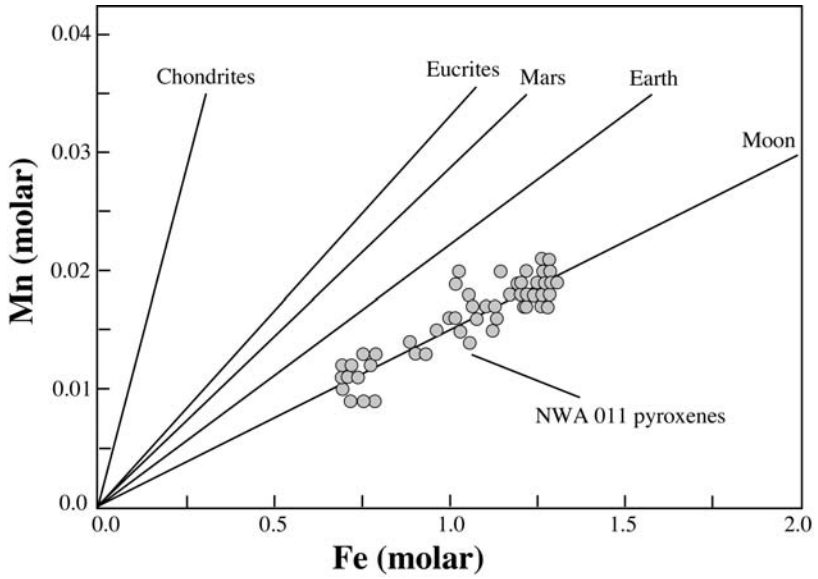

Fig. 3. Molar Fe versus Mn in pyroxenes from NWA 011. The Fe/Mn ratios are significantly higher than those of typical eucrites. Correlation lines are based on data from Papike (1998).

Table 3 and Fig. 4. The average isotopic composition of the four aliquots of NWA 011 that we measured is $\delta^{18}O = 2.92 \pm 0.22$ and $\delta^{17}O = -0.06 \pm 0.12$, consistent with the results of Yamaguchi et al. (2002). These data confirm that NWA 011 has an unusual oxygen isotopic composition that is far removed from the known eucrite field ($\Delta^{17}O = -1.58$ for NWA 011 versus −0.25 for the eucrites). The oxygen isotopic composition falls within the range of values observed for CR chondrites (Fig. 4), but is not like that of any other known achondrites (Clayton 1993; Clayton and Mayeda 1996).

Minor and trace element compositions of plagioclase, pyroxene and merrillite are given in Table 4, and the REE patterns are shown in Fig. 5. Two plagioclase grains have parallel LREE-enriched patterns with large positive Eu anomalies (Fig. 5a); REE abundances differ by about 50% between the two grains. Four merrillite grains have virtually identical REE abundances. The patterns are LREE-enriched with negative Eu anomalies; all four grains also show small positive Ce anomalies (Fig. 5b). The REE abundances in pyroxene are uniform, indicating that we adequately sampled both the augite lamellae and host pigeonite compositions. Moreover, we did not observe any core to rim zoning in three

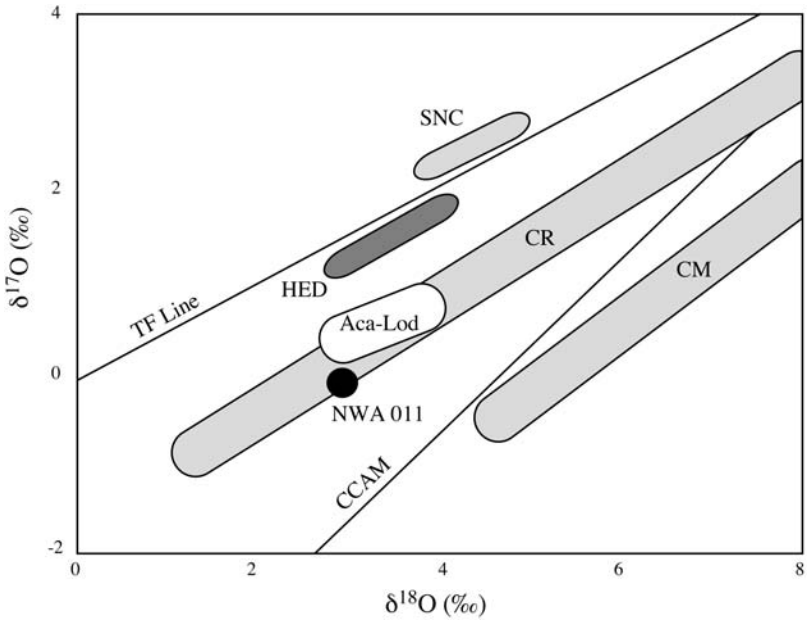

Fig. 4. Three isotope plots showing the oxygen isotopic composition of NWA 011 (black circle). Errors (0.22 ‰ for $\delta^{18}O$ and 0.12 ‰ for $\delta^{17}O$; 1σ) are smaller than the size of the symbol. Also shown are the terrestrial fractionation (TF) line, the carbonaceous chondrite anhydrous mineral (CCAM) line and the fields for CR chondrites, CM chondrites, Martian meteorites (SNC), the HED (howardite-eucrite-diogenite) meteorites and the acapulcoites/lodranites (Aca-Lod). Fields for meteorites other than NWA 011 are from Clayton (2003) and references therein.

Table 3. Oxygen isotopic data for NWA 011.

Aliquot	$\delta^{18}O$	$\delta^{17}O$
A1	3.23	0.10
A2	2.84	–0.10
B1	2.88	–0.08
B2	2.71	–0.17
Average	2.92 ± 0.22	–0.06 ± 0.12

pyroxene grains (Figs. 5c–e), consistent with the largely uniform major element compositions of the pigeonite (Table 2; Yamaguchi et al. 2002).

DISCUSSION

NWA 011 was originally classified as a non-cumulate eucrite and, indeed, this meteorite seems to share many similarities with the eucrites, including texture, mineralogy, and major element compositions, except for higher Fe/Mn ratios (e.g., Yamaguchi et al. 2002). In portions of the following discussion, therefore, we will compare the trace element data of NWA 011 with that of certain non-cumulate eucrites in order to elucidate its crystallization (and post-crystallization) history.

Ce Anomalies in Merrillite: Terrestrial Weathering?

Because NWA 011 is a meteorite recovered from a hot desert, terrestrial alteration and its possible effect on trace element compositions must be evaluated. Recent studies have shown that hot desert meteorites are quite susceptible to terrestrial contamination (Bland et al. 1996; Dreibus et al. 2001; Crozaz and Wadhwa 2001) and may experience significant chemical changes that can include enrichments of Rb, Sr, Ba, LREE, U, and Th, decreased abundances of C, N, and H, the presence of occasional Ce anomalies, and the addition of terrestrial noble gases (Scherer et al. 1994; Ash and Pillinger 1995; Barrat et al. 1999; Crozaz et al. 2003).

The evidence for terrestrial alteration of NWA 011 is mixed. Yamaguchi (2001) notes that the rock is quite weathered, but although Korochantseva et al. (2003) observed significant terrestrial Ar in their analysis of NWA 011, they also found that Ba and Sr abundances were low, indicating little to no contamination of these elements from the desert environment. Our data also do not show elevated abundances of Sr and Ba. However, we do observe small positive Ce anomalies in the four grains of merrillite measured here (Table 4, Fig. 4), although plagioclase and pyroxene grains do not exhibit any Ce anomalies. Cerium anomalies in minerals from hot desert meteorites are generally associated with LREE enrichments and are most often found in phases with low abundances of the LREE, such as olivines and pyroxenes (Crozaz et al. 2003). An exception is the brachinite Eagles Nest, which shows an LREE enrichment and large Ce depletion in apatite (Swindle et al. 1998; Crozaz et al. 2003). However, both olivine and whole rock analyses of this meteorite show the same features, indicating that this meteorite is strongly contaminated. Excesses in Ce could be produced through the oxidation of Ce (III) to Ce (IV) (e.g.,

Mittlefehldt and Lindstrom 1991), which is more insoluble than trivalent Ce. Dissolution of the Ca phosphates during aqueous alteration would result in the preferential retention of Ce (IV) relative to the trivalent REE, leading to positive Ce anomalies such as those observed in NWA 011. Although we find it unlikely that REE-rich Ca-phosphate would be affected by this process, while phases with lower REE concentrations, such as plagioclase and pyroxene, are not, we cannot rule out that terrestrial weathering is responsible for the Ce anomalies observed in NWA 011 merrillite. Moreover, Schreiber et al. (1980) have shown experimentally that Ce (IV) in magmatic systems will be reduced by Fe (II) to Ce (III). These authors note that "it is difficult to visualize a magma under realistic conditions where the Ce (IV) species would be stabilized." Thus, we conclude that the Ce anomalies in merrillite are not primary, but could be a secondary feature due to terrestrial alteration. However, other trace element compositions in NWA 011 do not appear to have been compromised by terrestrial contamination.

Bulk Compositions of NWA 011

Whole rock REE compositions of NWA 011 were calculated using the averages of our mineral compositions (Table 4) and the modes reported in Table 1. For the purposes of this calculation, the REE abundances in olivine, silica, and opaque minerals were assumed to be negligible. Figure 6 shows the three calculated bulk REE patterns together with the average mineral compositions of NWA 011. All three patterns are approximately flat to slightly LREE-enriched, with abundances of ~10 × CI and have small positive Eu anomalies. The patterns also have small positive Ce anomalies that reflect the influence of phosphate on the bulk composition of the meteorite. The REE pattern for bulk 1 has LREE abundances that are about a factor of two higher than those of bulk 2 and bulk 3, largely due to the higher modal abundance of Ca-phosphate in this thin section (Table 1).

Published whole rock REE patterns for NWA 011, however, are heterogeneous and differ from those calculated here. Both Yamaguchi et al. (2002) and Korotchantseva et al. (2003) analyzed chips of NWA 011, the REE patterns of which are HREE-enriched with large positive Eu anomalies. These REE patterns can be reproduced by assuming modal proportions of plagioclase and pyroxene with little to no Ca-phosphate (Fig. 7a). Another chip analyzed by Korotchantseva et al. (2003) has a LREE-rich pattern with a positive Ce anomaly and is clearly dominated by excess Ca-phosphate (Fig. 7b). Moreover, the negative Eu anomaly in this pattern requires a much larger fraction of pyroxene (and correspondingly less plagioclase) than is present in our sections (~88% versus 55–58%).

Table 5 shows two whole rock major element compositions for NWA 011 from the literature. Whole rock Y was determined by Yamaguchi et al. (2002) using wet chemical analysis, whereas whole rock K was determined by Korochantseva et al. (2003) using mineral chemistry and the mode published by Promprated et al. (2003) (i.e., mode 2 in Table 1). We also calculated bulk compositions from modes 1, 2, and 3 in Table 1 and the mineral compositions from Table 2 in order to compare them with the literature whole rock compositions. For the purposes of these calculations, we assumed that the proportions of augite to pigeonite and ilmenite to ulvöspinel were 1:2. The results are shown in Table 5. Our calculated bulk compositions generally show differences that are similar in magnitude to those between the two literature whole rock compositions and that are consistent with the differences in the three modes of Table 1. Thus, for example, bulk 1 has the highest concentrations of Al_2O_3, CaO, and Na_2O, consistent with the fact that this mode has the highest proportion of plagioclase. Similarly, the bulk composition calculated from mode 2, which has the highest proportion of pyroxene, has the highest concentrations of MgO and FeO. Concentrations of SiO_2 are intermediate between the whole rock values of Korochantseva et al. (2002) and Yamaguchi et al. (2002) and, not surprisingly, are highest in the two that contain silica in the mode. Moreover, all three of our calculated bulk compositions have somewhat higher Al_2O_3, CaO and Na_2O, and lower FeO and MgO than the whole rock determinations Y and K. Since the modal abundances for whole rock K and bulk 2 are the same, some of these differences must reflect the average mineral compositions used to calculate the bulk compositions. However, modes 1 and 3 also have more plagioclase than mode 2. Whole rock composition Y from Yamaguchi et al. (2002) has the highest MgO and FeO abundances and the lowest SiO_2, which seems to indicate a higher proportion of olivine in this analysis. The compositions calculated from mode 2, determined over the largest area of NWA 011 (Table 1), are most similar to the whole rock determination of Yamaguchi et al. (2002); this mode may be the most representative of NWA 011.

Equilibrium Melt Compositions and Crystallization History

If plagioclase and pyroxene in NWA 011 have preserved their original igneous signatures, it should be possible to calculate the REE compositions of the melts from which they crystallized. Although textural evidence and the uniformity of major element compositions in both plagioclase and pyroxene suggest that NWA 011 has undergone some re-equilibration, such a calculation can still provide some useful constraints on the nature of the NWA 011 parent melt, as well as possible secondary processes that may have affected the sample.

The distribution coefficients listed in Table 6 were used to calculate the compositions of liquids in equilibrium with core plagioclase and pyroxene grains from NWA 011. The D

Table 4. Minor and trace element concentrations (ppm) in NWA 011 minerals.

	Plagioclase 1	Plagioclase 2	Pyroxene 1–2 (core)	Pyroxene 1–2 (rim)	Pyroxene 3–4 (core)	Pyroxene 3–4 (rim)	Pyroxene 5–6 (core)
Na	n.d.	n.d.	320 ± 1	365 ± 2	380 ± 1	310 ± 1	340 ± 1
Mg	225 ± 2	485 ± 3	n.d.	n.d.	n.d.	n.d.	n.d.
P	340 ± 3	795 ± 4	1040 ± 5	1140 ± 9	670 ± 4	525 ± 4	645 ± 4
K	460 ± 1	585 ± 2	24 ± 1	39 ± 1	46 ± 1	26 ± 1	27 ± 1
Ca	n.d.	n.d.	n.d.	n.d.	n.d.	n.d.	n.d.
Sc	3.1 ± 0.2	4.6 ± 0.2	28 ± 1	25 ± 1	23 ± 1	23 ± 1	23 ± 1
Ti	100 ± 1	100 ± 1	2150 ± 4	2200 ± 7	2670 ± 5	2320 ± 4	2190 ± 4
Mn	84 ± 1	98 ± 1	5320 ± 6	5150 ± 10	4900 ± 6	5020 ± 6	4860 ± 6
Fe	4560 ± 35	17190 ± 75	n.d.	n.d.	n.d.	n.d.	n.d.
Sr	220 ± 1	225 ± 1	2.6 ± 0.1	5.3 ± 0.2	6.0 ± 0.2	4.1 ± 0.1	5.6 ± 0.1
Y	0.31 ± 0.02	0.97 ± 0.05	5.6 ± 0.1	5.0 ± 0.2	4.8 ± 0.1	5.2 ± 0.1	5.3 ± 0.1
Zr	0.30 ± 0.03	0.48 ± 0.04	11 ± 1	24 ± 1	28 ± 1	21 ± 1	23 ± 1
Ba	62 ± 1	85 ± 1	2.6 ± 0.1	7.3 ± 0.4	9.9 ± 0.3	6.5 ± 0.3	7.8 ± 0.3
La	0.28 ± 0.02	0.54 ± 0.04	0.086 ± 0.010	b.d.	0.10 ± 0.01	0.074 ± 0.010	0.10 ± 0.01
Ce	0.82 ± 0.05	1.0 ± 0.06	0.42 ± 0.03	0.39 ± 0.04	0.43 ± 0.03	0.41 ± 0.03	0.45 ± 0.03
Pr	0.069 ± 0.007	0.10 ± 0.01	0.11 ± 0.01	0.10 ± 0.01	0.074 ± 0.007	0.081 ± 0.007	0.11 ± 0.01
Nd	0.22 ± 0.01	0.34 ± 0.02	0.50 ± 0.02	0.42 ± 0.03	0.39 ± 0.02	0.45 ± 0.03	0.51 ± 0.02
Sm	0.052 ± 0.010	0.074 ± 0.014	0.26 ± 0.02	0.28 ± 0.04	0.25 ± 0.02	0.22 ± 0.02	0.26 ± 0.02
Eu	1.5 ± 0.1	1.6 ± 0.1	0.029 ± 0.006	0.039 ± 0.02	0.017 ± 0.013	0.025 ± 0.010	0.041 ± 0.010
Gd	0.037 ± 0.010	0.080 ± 0.014	0.40 ± 0.04	0.26 ± 0.06	0.34 ± 0.03	0.45 ± 0.04	0.35 ± 0.04
Tb	0.0076 ± 0.0023	0.0084 ± 0.0038	0.083 ± 0.007	0.092 ± 0.014	0.083 ± 0.009	0.089 ± 0.007	0.10 ± 0.01
Dy	0.040 ± 0.006	0.09 ± 0.01	0.79 ± 0.03	0.70 ± 0.04	0.62 ± 0.03	0.82 ± 0.03	0.76 ± 0.03
Ho	b.d.	b.d.	0.19 ± 0.01	0.15 ± 0.02	0.15 ± 0.01	0.19 ± 0.01	0.17 ± 0.01
Er	b.d.	b.d.	0.64 ± 0.02	0.56 ± 0.04	0.55 ± 0.03	0.67 ± 0.02	0.61 ± 0.02
Tm	b.d.	b.d.	0.11 ± 0.01	0.098 ± 0.010	0.096 ± 0.009	0.099 ± 0.007	0.11 ± 0.01
Yb	0.017 ± 0.006	0.023 ± 0.009	0.68 ± 0.04	0.77 ± 0.07	0.67 ± 0.05	0.91 ± 0.04	0.80 ± 0.04
Lu	b.d.	b.d.	0.13 ± 0.01	0.13 ± 0.02	0.14 ± 0.01	0.15 ± 0.01	0.10 ± 0.01
Eu/Eu[a]	97	62	0.27	0.43	0.17	0.24	0.41
Ce/Ce[a]							

[a]Errors are 1σ from counting statistics only.
n.d. = not determined; b.d. = below detection.

Table 4. *Continued.* Minor and trace element concentrations (ppm) in NWA 011 minerals.

	Pyroxene 5-6 (rim)	Pyroxene 7 (core)	Pyroxene 8 (core)	Merrillite 1	Merrillite 2	Merrillite 3	Merrillite 4
Na	275 ± 1	605 ± 2	340 ± 1	n.d.	n.d.	n.d.	n.d.
Mg	n.d.	n.d.	n.d.	n.d.	n.d.	n.d.	n.d.
P	455 ± 3	2000 ± 10	895 ± 6	n.d.	n.d.	n.d.	n.d.
K	13 ± 1	93 ± 1	27 ± 1	n.d.	n.d.	n.d.	n.d.
Ca	n.d.	n.d.	n.d.	n.d.	n.d.	n.d.	n.d.
Sc	22 ± 1	32 ± 1	26 ± 1	n.d.	n.d.	n.d.	n.d.
Ti	2810 ± 4	2620 ± 7	1810 ± 5	n.d.	n.d.	n.d.	n.d.
Mn	4950 ± 5	5660 ± 9	5020 ± 8	n.d.	n.d.	n.d.	n.d.
Fe	n.d.	n.d.	n.d.	n.d.	n.d.	n.d.	n.d.
Sr	3.7 ± 0.1	6.8 ± 0.2	4.6 ± 0.2	n.d.	n.d.	n.d.	n.d.
Y	4.9 ± 0.1	4.6 ± 0.2	5.7 ± 0.2	n.d.	n.d.	n.d.	n.d.
Zr	32 ± 1	28 ± 1	12 ± 1	n.d.	n.d.	n.d.	n.d.
Ba	4.4 ± 0.2	10 ± 1	9.4 ± 0.4	n.d.	n.d.	n.d.	n.d.
La	0.068 ± 0.009	0.13 ± 0.02	0.069 ± 0.015	290 ± 3	290 ± 3	320 ± 4	260 ± 5
Ce	0.44 ± 0.03	0.44 ± 0.05	0.51 ± 0.04	1310 ± 7	1270 ± 8	1390 ± 8	100 ± 11
Pr	0.071 ± 0.006	0.091 ± 0.011	0.11 ± 0.01	130 ± 2	145 ± 2	150 ± 3	115 ± 3
Nd	0.42 ± 0.02	0.42 ± 0.03	0.52 ± 0.03	490 ± 5	510 ± 5	540 ± 6	425 ± 8
Sm	0.22 ± 0.01	0.19 ± 0.02	0.27 ± 0.03	120 ± 4	125 ± 4	140 ± 5	100 ± 5
Eu	0.038 ± 0.007	0.046 ± 0.018	0.056 ± 0.018	14 ± 1	13 ± 1	16 ± 1	12 ± 1
Gd	0.32 ± 0.02	0.35 ± 0.04	0.55 ± 0.05	110 ± 4	115 ± 4	115 ± 5	92 ± 6
Tb	0.080 ± 0.005	0.082 ± 0.010	0.11 ± 0.01	20 ± 1	23 ± 1	23 ± 1	16 ± 2
Dy	0.70 ± 0.02	0.64 ± 0.04	0.89 ± 0.04	120 ± 3	120 ± 3	130 ± 3	115 ± 3
Ho	0.16 ± 0.01	0.13 ± 0.02	0.19 ± 0.02	24 ± 1	24 ± 1	26 ± 1	23 ± 1
Er	0.58 ± 0.02	0.58 ± 0.03	0.70 ± 0.04	59 ± 2	65 ± 2	64 ± 2	50 ± 2
Tm	0.10 ± 0.01	0.10 ± 0.01	0.10 ± 0.01	8.1 ± 0.5	8.4 ± 0.5	8.1 ± 0.6	8.2 ± 0.6
Yb	0.75 ± 0.03	0.74 ± 0.05	0.82 ± 0.05	37 ± 2	40 ± 2	41 ± 2	35 ± 2
Lu	0.13 ± 0.01	0.12 ± 0.02	0.15 ± 0.02	4.8 ± 0.5	3.5 ± 0.5	4.8 ± 0.6	4.0 ± 0.5
Eu/Eu[a]	0.43	0.54	0.43	0.36	0.33	0.38	0.38
Ce/Ce[a]				1.60	1.49	1.51	1.53

[a]Errors are 1σ from counting statistics only.

n.d. = not determined; b.d. = below detection.

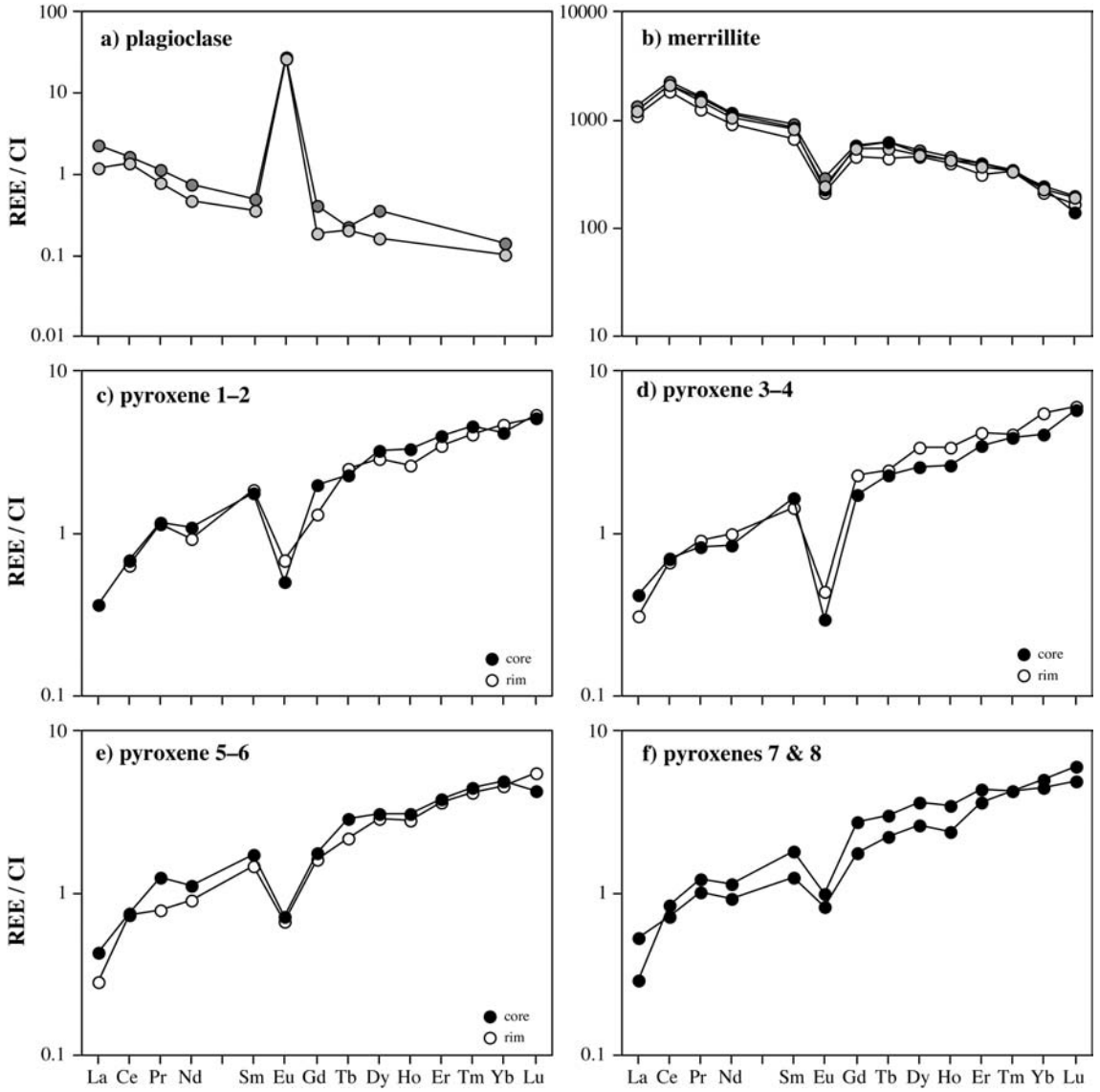

Fig. 5. CI chondrite-normalized REE patterns of minerals in NWA 011: a) core analyses of two plagioclase grains; b) analyses of four different merrillite grains; c–e) core and rim analyses of three pyroxene grains; f) core analyses of two pyroxene grains.

Table 5. Whole rock major element concentrations (in wt%) for NWA 011.

	Whole rock Y[a]	Whole rock K[b]	Bulk 1	Bulk 2	Bulk 3	Average bulk
SiO_2	45.63	48.22	46.69	47.20	47.75	47.66
TiO_2	0.92	0.85	0.43	0.67	0.52	0.54
Cr_2O_3	0.24	0.19	0.15	0.18	0.16	0.16
Al_2O_3	13.12	12.86	15.07	13.69	14.54	14.55
FeO	21.13	19.95	18.02	19.34	18.26	18.45
MnO	0.40	0.29	0.28	0.29	0.27	0.28
MgO	6.66	6.05	5.16	5.48	5.19	5.26
CaO	11.11	10.76	12.31	11.58	11.74	11.93
Na_2O	0.45	0.54	0.73	0.67	0.71	0.71
K_2O	0.03	0.03	0.03	0.03	0.03	0.03
P_2O_5	<0.02	0.22	0.50	0.23	0.18	0.30
Total	99.71	99.96	99.35	99.33	99.35	99.87

[a] Y: Yamaguchi et al. (2002), wet chemical analysis;

[b] K: Korochantseva et al. (2003), calculated composition (see text).

Bulks 1, 2, and 3 calculated from modes 1, 2, and 3 of Table 1 and mineral compositions from Table 2.

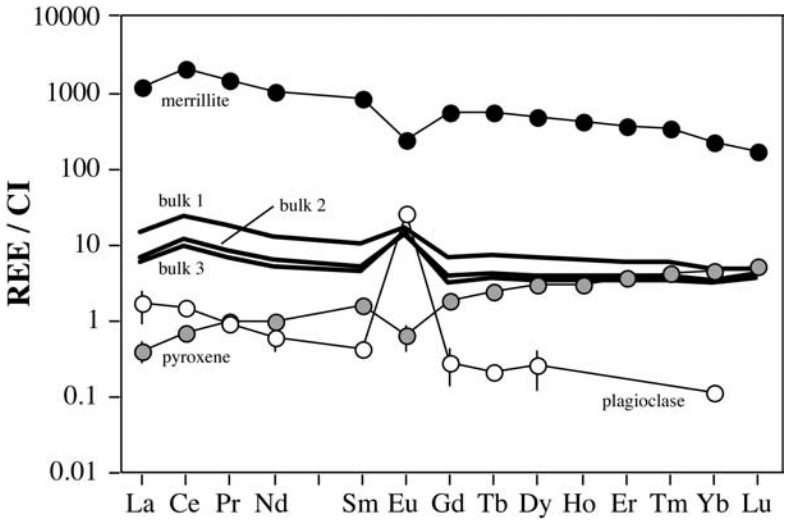

Fig. 6. CI chondrite-normalized bulk REE patterns for NWA 011 along with the average mineral REE patterns used to calculate the whole rock compositions. Bulks 1, 2, and 3 correspond to the respective modes listed in Table 1.

values used for pyroxene were calculated from the parameters given by McKay et al. (1986) for pigeonite of Wo_{20} composition, which approximates the average CaO content of NWA 011 pyroxene reconstructed from the pigeonite and augite lamellae. Figure 8 shows the REE patterns of the liquids in equilibrium with plagioclase 1 and the core of pyroxene 3–4 (Table 4) together with the average bulk composition of NWA 011 calculated from the mineral data. Both parent melt compositions have approximately flat to slightly LREE-enriched REE patterns at ~20 × CI, indicating that the two minerals crystallized from similar melts. The REE pattern for the melt in equilibrium with plagioclase has a small positive Eu anomaly, similar to that seen in the bulk REE pattern, suggesting that this feature is real and is not simply an artifact reflecting an overabundance of plagioclase in the mode determined from our thin sections. The melt REE patterns for both pyroxene and plagioclase are approximately parallel to the bulk REE pattern, but have somewhat elevated abundances, particularly for the HREE. Moreover, the melt calculated to be in equilibrium with pyroxene is somewhat LREE-enriched relative to the bulk pattern. This enrichment probably reflects homogenization of the REE within originally zoned grains. In plagioclase, equilibration of the REE will tend to increase REE abundances, relative to the original core compositions, without significantly affecting the shape of the pattern; equilibration of the REE in pyroxene will, in addition, tend to increase the LREE abundances (for detailed discussions of the effects of equilibration on REE abundances and patterns in minerals, see Hsu and Crozaz [1996] and Floss et al. [1998]). Thus, the REE composition of the original parent melt for NWA 011 was probably quite similar to the average bulk REE pattern shown in Fig. 8. The effects of thermal metamorphism on the trace element compositions of NWA 011 minerals will be discussed in more detail below.

The whole rock major element compositions of NWA 011 (K and Y; Table 5) were used with the MELTS program to model the crystallization of NWA 011 at an fO_2 of IW. Figure 9 shows that equilibrium crystallization from the bulk composition of Korotchantseva et al. (2003) results in a crystallization sequence of pigeonite + plagioclase → spinel → olivine → augite → merrillite → ilmenite → silica. The crystallization order from the bulk composition of Yamaguchi et al. (2002) is slightly different (spinel → plagioclase → olivine → pigeonite → augite → merrillite) and lacks primary ilmenite and silica. These differences are probably due to sample heterogeneity for the determination of bulk compositions, as discussed above for the bulk REE compositions. For example, the earlier crystallization of spinel from whole rock Y probably reflects the higher concentrations of Fe and Cr in this bulk composition because spinel stability is very sensitive to Cr contents. Both compositions indicate extensive co-crystallization of plagioclase and pigeonite, consistent with the REE parent melt compositions calculated above. However, both also predict significant augite crystallization after the onset of pigeonite crystallization, although no augite is present in our section. Yamaguchi et al. (2002) did note the presence of relict augite grains in their section of NWA 011, but did not give an estimate of their abundance. In addition, pigeonite compositions show a large range in Fe/Mg that is not seen in our mineral compositions (Table 2); post-crystallization processes are probably responsible for the equilibration of pyroxene compositions in NWA 011.

Metamorphism on the NWA 011 Parent Body

Other evidence also suggests that thermal metamorphism has played a role in the evolution of NWA 011. Yamaguchi et al. (2002) noted that NWA 011 exhibits a number of

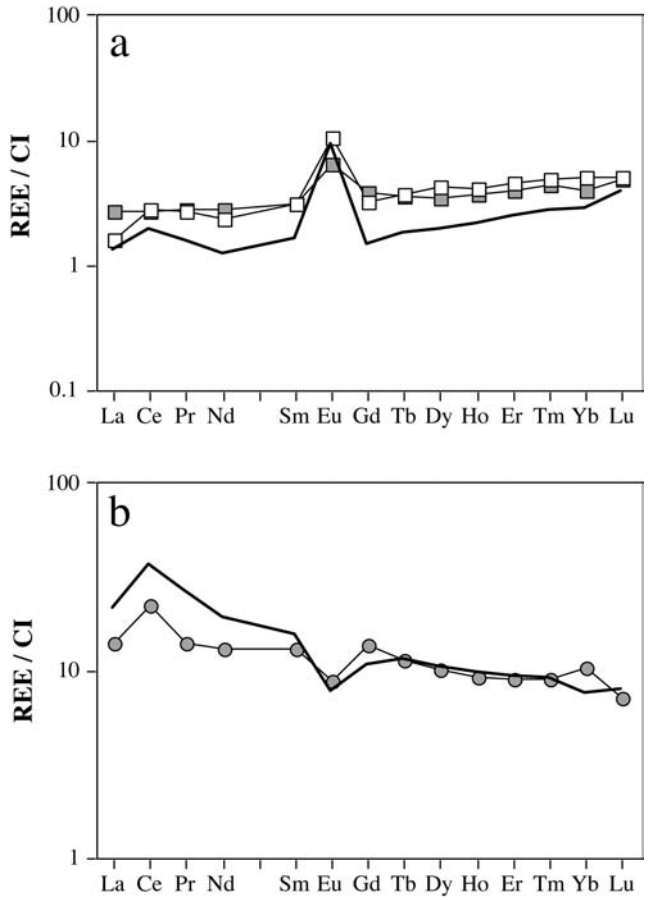

Fig. 7. CI chondrite-normalized bulk REE patterns for NWA 011. The white symbols are data from Yamaguchi et al. (2002), the grey symbols are data from Korotchantseva et al. (2003), and the solid lines represent patterns calculated from the mineral compositions measured in this study. a) HREE-rich patterns can be reproduced using 58.5% pyroxene, 39.6% plagioclase (Table 1), and = 0.05% Ca-phosphate; b) the LREE-enriched pattern can be reproduced using 88% pyroxene, 10% plagioclase, and 1.6% Ca-phosphate.

mineralogical features seen in highly metamorphosed eucrites, such as Ibitira, EET 90020, and Y-86763 (Floss et al. 2000; Yamaguchi et al. 2001). The low-Ca pyroxene in NWA 011 consists of pigeonite with fine exsolution lamellae of augite, similar to equilibrated pyroxenes in type 5 eucrites (Takeda and Graham 1991). Application of the two-pyroxene thermometer of Kretz (1982) indicates an equilibration temperature of ~860 °C, whereas the compositions of relict augite and pigeonite observed by Yamaguchi et al. (2002) suggest a peak metamorphic temperature of ~1090–1100 °C. NWA 011 also contains oxide assemblages (ilmenite and Ti-rich chromite) associated with Fe-rich olivine and pyroxene (e.g., Fig. 1b). In the highly equilibrated eucrites, such features, which are not in equilibrium with the rest of the meteorite, have been attributed to a rapid reheating and cooling event following thermal metamorphism on the eucrite parent body (Floss et al. 2000; Yamaguchi et al. 2001).

In a study of trace element distributions in eucrites, Hsu and Crozaz (1996) showed that pyroxene and plagioclase from many non-cumulate eucrites have LREE/HREE ratios that fall along a single correlation line. For plagioclase, this line also represents the abundances expected for crystallization from melts with chondritic proportions of the REE. However, these authors, as well as Floss et al. (2000), noted that some highly metamorphosed eucrites have plagioclase and pyroxene compositions that are LREE-enriched and thus fall to the right of these lines. Figure 10 plots the LREE/HREE ratios of plagioclase and pyroxene from NWA 011 relative to the correlation lines seen in non-cumulate eucrites. NWA 011 plagioclase falls on the non-cumulate eucrite line, suggesting that it crystallized from a chondritic melt. Pyroxene from NWA 011, however, falls somewhat to the right of the line. In the highly metamorphosed eucrites studied by Hsu and Crozaz (1996) and Floss et al. (2000), the LREE enrichments observed in plagioclase and pyroxene were attributed to extensive redistribution of the REE between Ca-phosphates and the silicate minerals, possibly due to partial melting of mesostasis material, which contains the phosphates, and interaction of this melt with plagioclase and pigeonite to produce the LREE-enriched signature. It is unlikely that a similar process accounts for the LREE-rich nature of NWA 011 pyroxene, because such a mechanism would be expected to enrich both silicate minerals. A more likely explanation is that homogenization of the REE within originally zoned pyroxene grains during thermal metamorphism accounts for the observed LREE enrichment. This is consistent with the observation above that equilibrium melt compositions calculated for pyroxene are LREE-enriched relative to those determined for plagioclase. Moreover, the fact that plagioclase LREE/HREE ratios fall on the non-cumulate correlation line, while pyroxene ratios do not, suggests that redistribution of the REE was limited to intra-grain re-equilibration and did not involve redistribution between mineral grains.

The distributions of other trace elements in NWA 011 plagioclase and pyroxene, relative to eucrites, are shown in

Table 6. Partition coefficients used to calculate NWA 011 equilibrium melts.

	Plagioclase[a]	Pigeonite (Wo_{20})[b]
La	0.051 ± 0.010	0.007 ± 0.003
Ce	0.044 ± 0.009	0.014 ± 0.005
Nd	0.038 ± 0.008	0.055 ± 0.015
Sm	0.031 ± 0.006	0.106 ± 0.018
Eu	1.15 ± 0.23	
Gd	0.021 ± 0.004	0.129 ± 0.036
Yb	0.0038 ± 0.0008	0.238 ± 0.029
Lu		0.242 ± 0.029

[a]Data from Jones (1995);
[b]Data from McKay et al. (1986)
Errors are estimated at 20% relative for plagioclase and are the average relative errors given by McKay et al. (1986) for pigeonite.

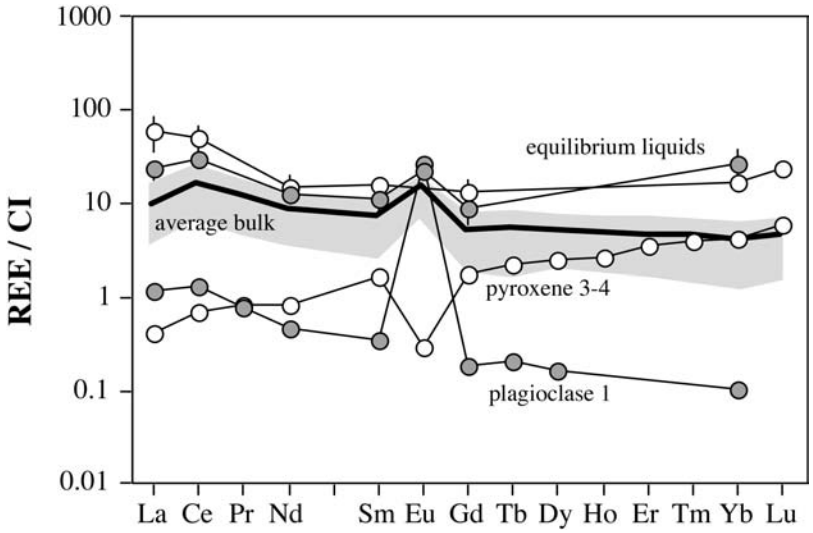

Fig. 8. CI chondrite-normalized REE patterns for liquids calculated to be in equilibrium with plagioclase (grey symbols) and pyroxene (white symbols) from NWA 011. Also shown (solid line) is the REE pattern calculated from the average modal composition (Table 1); the shaded area shows 1 errors.

Figs. 11 and 12. Sodium, Ba, Sr, and K abundances in NWA 011 plagioclase generally fall within or near the fields previously defined for non-cumulate eucrites (Hsu and Crozaz 1996). This is also true for the highly metamorphosed eucrites EET 90020 and Y-86763, an observation that led Floss et al. (2000) to suggest that abundances of these trace elements in plagioclase had not been affected by inter-mineral redistribution, despite the fact that the REE had been affected. For NWA 011, the similarities provide another link of this meteorite to the eucrites. The abundances of Ti, Y, and Zr in pyroxene from NWA 011 are intermediate between those in non-cumulate eucrites and those in highly metamorphosed eucrites (Fig. 12). This implies some redistribution of these elements in NWA 011 pyroxene, although it seems to have been more limited in NWA 011 than in Ibitira, EET 90020, and Y-86763. Alternatively, it could simply reflect primary source differences. In summary, if NWA 011 can be compared with the eucrites, it appears that although thermal metamorphism resulted in some REE redistribution in NWA 011 pyroxene, overall the effects on trace element compositions are less than in some of the highly metamorphosed eucrites. In particular, there is no clear evidence for any partial melting and resultant redistribution of the REE from phosphates to silicate minerals.

Did NWA 011 Originate on the Eucrite Parent Body?

We have repeatedly noted the many similarities that NWA 011 bears to the eucrites. The mineralogy and textures seen in NWA 011 are like those of some highly metamorphosed eucrites (e.g., Yamaguchi et al. 2002) and major element mineral compositions resemble those of non-cumulate eucrites (e.g., Fig. 2). As we have seen, the similarities also extend to trace element compositions. The whole rock REE composition of NWA 011 is around 10 × CI (Fig. 6), similar to those typically seen in eucrites (Consolmagno and Drake 1977), and silicate mineral REE abundances fall within the ranges seen in non-cumulate eucrites (Hsu and Crozaz 1996). Abundances of other trace elements are also like those of the non-cumulate eucrites (Figs. 11 and 12). Moreover, NWA 011 has a cosmic ray exposure age of 30 Ma (Yamaguchi et al. 2002), within the range of cosmic ray exposure ages for eucrites (7–70 Ma; Eugster and Michel 1995), and its Sm-Nd age of 4.46 ± 0.04 Ga is identical, within errors, to the age of 4.51 ± 0.04 determined for EET 90020 (Nyquist et al. 2003). ^{39}Ar-^{40}Ar data have been more difficult to interpret, due to the effects of significant weathering of this meteorite. Both Korotchantseva et al. (2003) and Bogard and Garrison (2004) report "ages" of ~3.2 Ga for the last major degassing event of NWA 011, which is outside of the time period in which the ^{39}Ar-^{40}Ar ages of most eucrites have been reset (~3.4–4.1 Ga; Bogard and Garrison 2003). However, Bogard and Garrison (2004) also noted that two whole rock analyses give higher maximum ages (within the eucrite range) at intermediate temperatures and pointed out that the space exposure age of NWA 011 is close to a peak in cosmic ray exposure ages observed in many other HED meteorites (Wakefield et al. 2004).

Despite these similarities, the oxygen isotopic composition of NWA 011 is clearly distinct from that of the HED meteorites and Fe/Mn ratios are higher than those of typical eucrites. Our trace element data suggest additional differences. Although most trace elements in plagioclase have abundances within the eucrite range, Sr abundances are slightly elevated relative to eucrites. Moreover, REE abundances in merrillite are lower by a factor of 10 than in typical eucrites and both pyroxene and phosphate have smaller Eu anomalies than most eucrites.

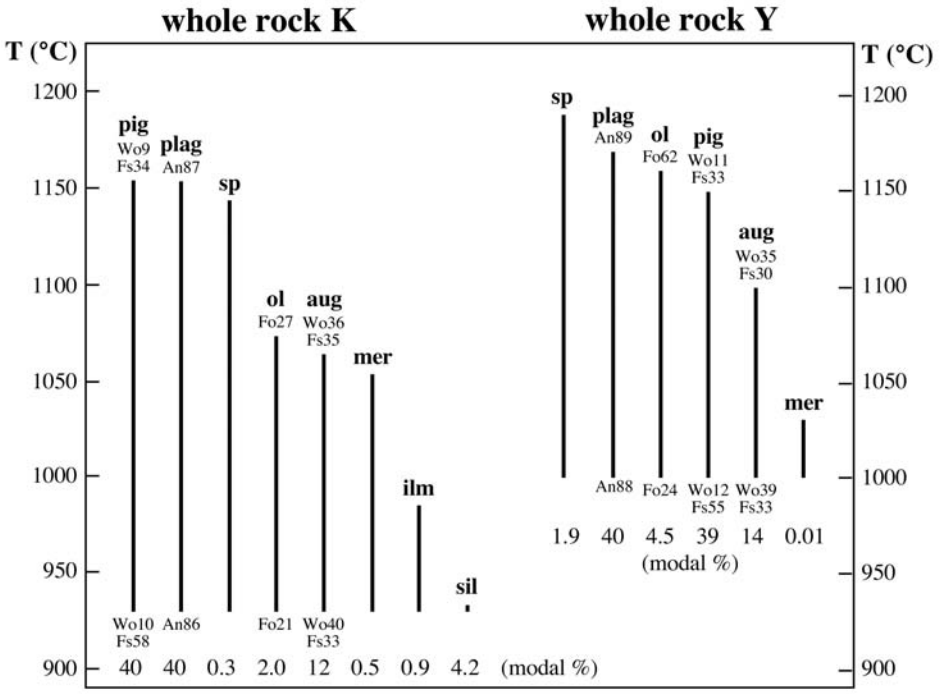

Fig. 9. Equilibrium crystallization sequences for NWA 011 whole rock compositions K and Y (Table 5): pig = pigeonite; plag = plagioclase; sp = spinel; ol = olivine; aug = augite; mer = merrillite; ilm = ilmenite; sil = silica.

In principle, infiltration of an Fe-rich metasomatizing liquid could account for the elevated Fe/Mn ratios in NWA 011 and some trace element features, such as the elevated Sr abundances in plagioclase. However, comparison of the whole rock compositions of NWA 011 (Table 2) with those from a variety of eucrites (Kitts and Lodders 1998) suggests that NWA 011 is, in fact, depleted in Mn relative to other eucrites and only shows a slight enrichment in Fe. Moreover, metasomatism would be expected to enrich all minerals in Fe, but plagioclase compositions show FeO concentrations within the ranges typically seen for eucrites. In addition, it is not clear how such a process might account for merrillite REE abundances that are 10× lower than in typical eucrites.

The most difficult characteristic of NWA 011 to reconcile with the eucrites, however, is its oxygen isotopic composition (Fig. 4), which falls far from the known eucrite field. Wiechert et al. (2002) have noted that eucrites exhibit oxygen isotopic heterogeneity and have suggested that the eucrites must come from at least four different parent bodies or from isotopically different reservoirs of the same planetary body. However, the total $\Delta^{17}O$ variation in oxygen isotopic composition measured by Wiechert et al. (2002) spans a range of −0.07 ‰ to −0.25 ‰, far less than the $\Delta^{17}O$ of −1.58 ‰ measured for NWA 011. This large difference makes it unlikely that NWA 011 comes from a previously unsampled isotopically heterogeneous reservoir on the eucrite parent body. Moreover, there are no known secondary processes that can produce such a change in oxygen isotopes. Thus, we conclude that NWA 011 did not originate on the HED parent body, despite the many similarities this meteorite exhibits with eucrites.

Is NWA 011 Related to the Acapulcoites–Lodranites?

The acapulcoites and lodranites are a group of related primitive achondrites that probably originated from the same parent body (Mittlefehldt et al. 1996; McCoy et al. 1996, 1997a). These meteorites experienced variable degrees of heating, resulting in complex partial melting and melt migration processes (McCoy et al. 1997b; Floss 2000). Lodranites are typically depleted in troilite and plagioclase and have lost ~15% or more silicate partial melts, relative to the acapulcoites, which have generally retained chondritic mineralogies. However, geochemical data show that the two groups are not always easily distinguished on petrographic criteria alone and that the acapulcoite/lodranite clan forms a continuum, exhibiting a range of degrees of heating and partial melting that may or may not be accompanied by melt migration (Floss 2000; Patzer et al. 2004). The oxygen isotopic composition of NWA 011 falls near that of the acapulcoites and lodranites (Fig. 4), raising the question of whether NWA 011 could be related to these meteorites. As noted above, the lodranites are residues that have lost silicate partial melts. However, with the possible exception of a coarse-grained lithology in the anomalous acapulcoite LEW 86220 (McCoy et al. 1997b), these basaltic partial melts have not been identified in the meteorite population. We

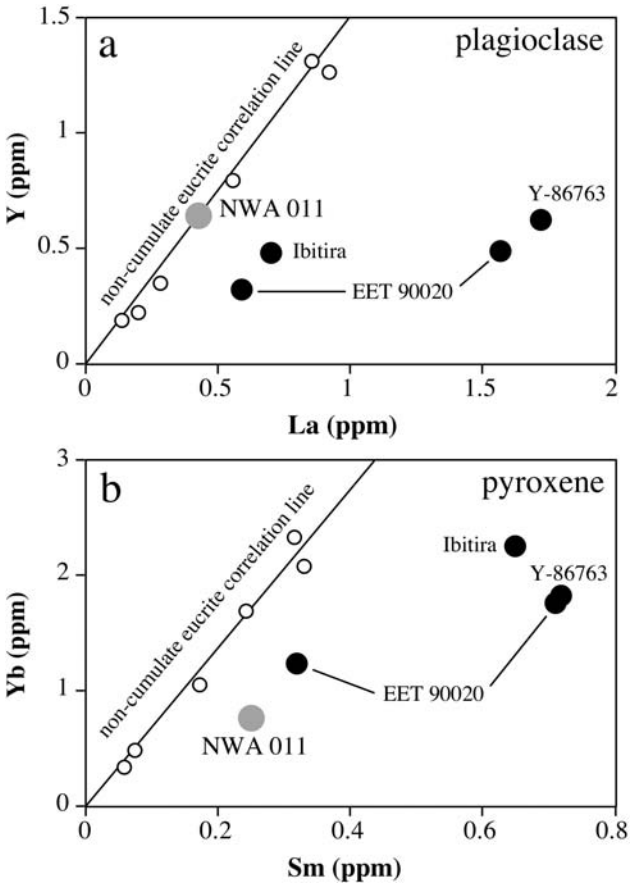

Fig. 10. Plots of a) La versus Y in plagioclase and b) Sm versus Yb in pigeonite from NWA 011 (grey symbols). The solid lines represent correlations of these elements observed in non-cumulate eucrites (white symbols). Highly metamorphosed eucrites (black symbols) experienced redistribution of the REE and fall to the right of the line. Eucrite data are from Hsu and Crozaz (1996), Floss et al. (2000), and Yamaguchi et al. (2001).

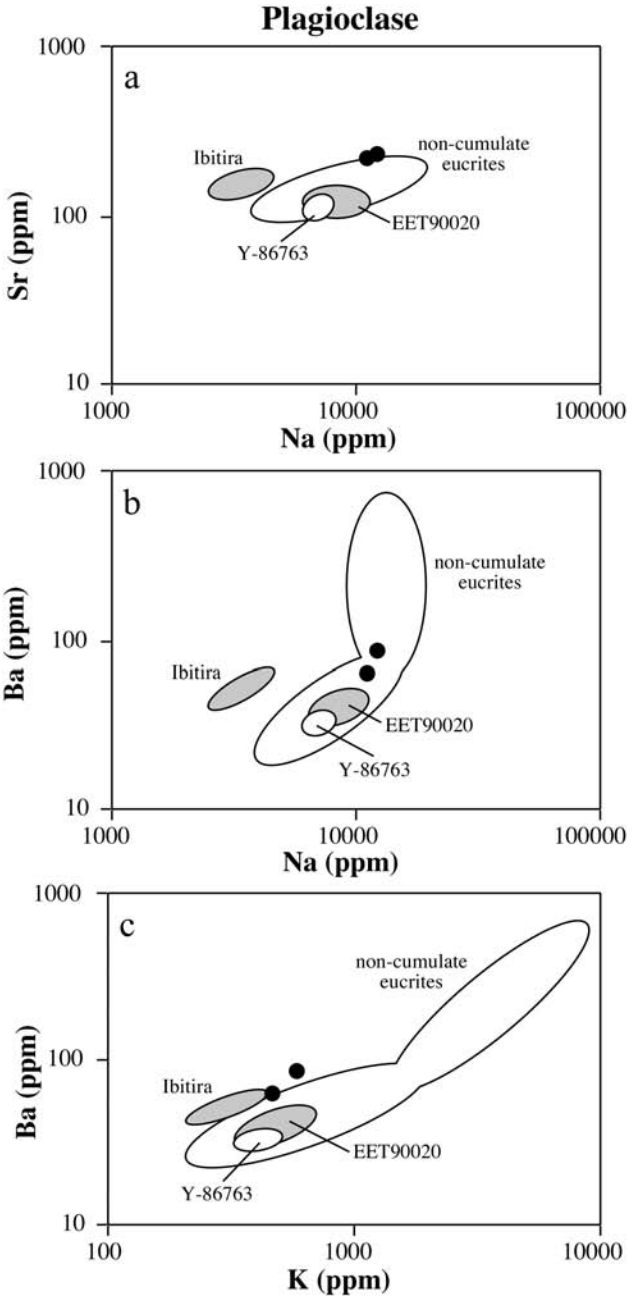

Fig. 11. Scatter plots of a) Na versus Sr; b) Na versus Ba; and c) K versus Ba in NWA 011 plagioclase (black symbols). Also shown are the fields for non-cumulate eucrites (Stannern, Nuevo Laredo, Sioux County, Pasamonte, Lakangaon, and Chervony Kut) and for the highly metamorphosed eucrites Ibitira, EET 90020, and Y-86763. Eucrite data are from Hsu and Crozaz (1996), Floss et al. (2000), and Yamaguchi et al. (2001).

investigate here whether NWA 011 could represent a sample of the basaltic partial melt complementary to the lodranite residues.

The first silicate melt to form through heating of a chondritic parent body should be enriched in incompatible elements and the trace elements associated with a feldspathic component. Such a melt is likely to be LREE-enriched and one would expect the minerals crystallizing from such a melt to be LREE-enriched, relative to those crystallizing from a melt with chondritic abundances of the REE. In fact, as we noted earlier, the parent melt composition calculated for NWA 011 is slightly LREE-enriched with a small positive Eu anomaly (Fig. 8). In addition, Fig. 13a shows that NWA 011 merrillite is distinctly LREE-rich compared to merrillite from the acapulcoites. However, plagioclase from NWA 011 has a flatter rather than steeper LREE pattern than plagioclase from the acapulcoites (Fig. 13b) and, as we noted earlier, NWA 011 plagioclase has LREE/HREE ratios that are consistent with crystallization from a chondritic source. Pyroxene REE compositions do not provide any information in this situation; LREE abundances in pyroxene vary with major element composition (e.g., Wo contents) and the pyroxenes present in the acapulcoites are orthopyroxene and augite, whereas those in NWA 011 are pigeonite. Thus, a direct comparison of REE abundances is not possible.

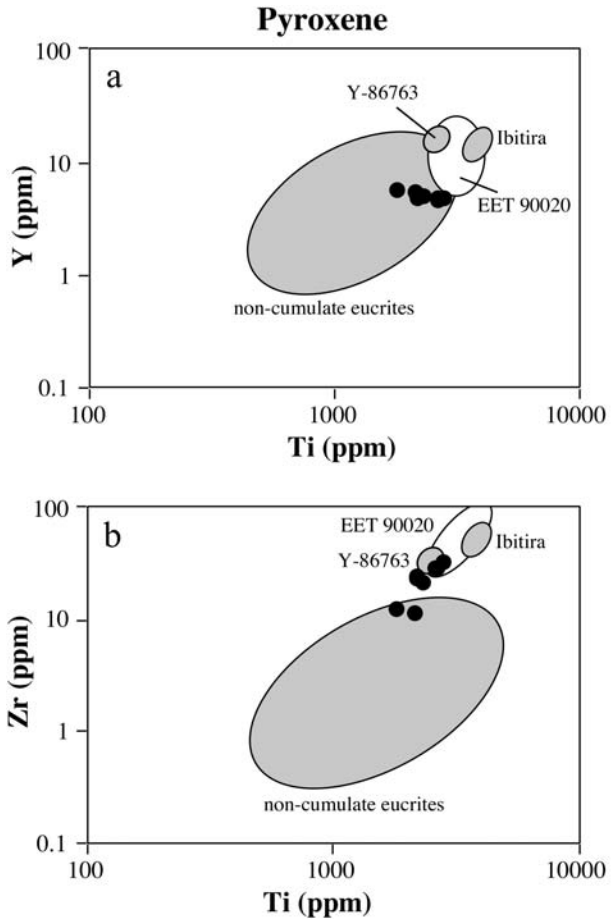

Fig. 12. Scatter plots of a) Ti versus Y and b) Ti versus Zr in NWA 011 pyroxene (black symbols). Also shown are the fields for non-cumulate eucrites (Stannern, Nuevo Laredo, Sioux County, Pasamonte, Lakangaon, and Chervony Kut) and for the highly metamorphosed eucrites Ibitira, EET 90020, and Y-86763. Eucrite data are from Hsu and Crozaz (1996), Floss et al. (2000), and Yamaguchi et al. (2001).

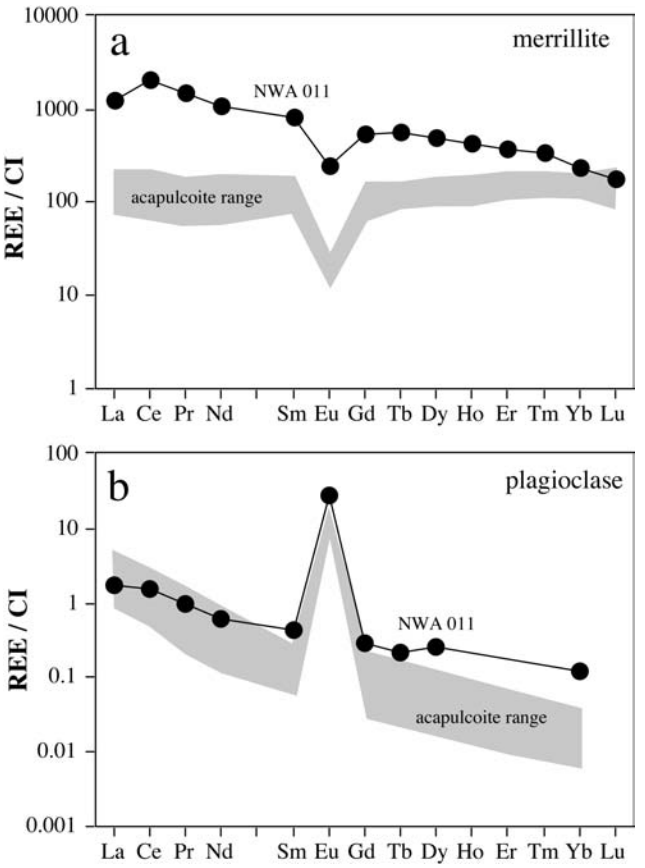

Fig, 13. CI chondrite-normalized REE patterns for a) merrillite and b) plagioclase from NWA 011. Shaded areas show the range of abundances observed in the acapulcoites (data from Floss 2000).

Despite the similarities noted here between the NWA 011 parent melt composition and the REE compositions expected for a basaltic partial melt from the acapulcoite/lodranite parent body, it is unlikely that NWA 011 is, in fact, a basaltic sample from the acapulcoite/lodranite parent body. NWA 011 has a very fractionated bulk composition, with a molar Fe/Mg ratio of about 1.8. Goodrich and Delaney (2000) have shown that low degrees of partial melting (2%) of a chondritic precursor will result in liquids that have higher Fe/Mg ratios than the bulk composition and slightly lower Fe/Mn. As the degree of melting increases, these ratios move back toward the original chondritic compositions. Fractional crystallization of these melts produces strong increases in the Fe/Mg ratio without much change in Fe/Mn ratios, while the resulting cumulates have lower Fe/Mg ratios (cf. Fig. 5 in Goodrich and Delaney 2000). Very high Fe/Mg ratios, such as those observed in NWA 011, cannot be produced through partial melting and thus are probably the result of a fractional crystallization process on its parent body. Such a scenario would also be consistent with the slightly fractionated parent melt composition that we calculated: crystallization and accumulation of mafic olivine and/or pyroxene would enrich the remaining melt in the LREE and could produce a small positive Eu anomaly, as we observe for NWA 011 (Fig. 8). In this context, Korotchantseva et al. (2003) noted that NWA 011 is depleted in Sc, suggesting pyroxene fractionation.

It is not feasible that extensive fractional crystallization, like that required to produce the Fe-rich composition of NWA 011, could have occurred on the acapulcoite/lodranite parent body, which has retained significant chondritic chemical and mineralogical characteristics. Mafic cumulates that would represent the counterpart to the fractionated basalt represented by NWA 011 have also not been sampled from the acapulcoite/lodranite parent body. In addition, siderophile element abundances in NWA 011 are highly fractionated (Yamaguchi et al. 2002; Korotchantseva et al. 2003), suggesting core formation, which has clearly not occurred on the acapulcoite/lodranite parent body. Thus, we conclude that NWA 011 is not genetically related to the acapulcoites and lodranites, despite the similarity in oxygen isotopes.

Relationship to CR Chondrites?

The oxygen isotopic composition of NWA 011 falls within the range noted for the CR chondrites. The CR chondrites are a group of fourteen meteorites named after the type member, Renazzo (Weisberg et al. 1993; Krot et al. 2002). They are generally of petrologic type 2 and contain abundant hydrous silicates. Despite the aqueous alteration they have experienced, they are considered to be highly primitive because the ratios of refractory lithophile elements to Mg abundances are similar to those of CI chondrites. Boesenberg (2003) modeled possible parent body compositions that, upon melting, would produce magmas consistent with the NWA 011 bulk composition; oxygen isotopic compositions were also constrained to match that of NWA 011. Several models, including H-Allende and a LL-Allende mixtures, produced compositions that were very similar to that of the bulk major element compositions of NWA 011. Surprisingly, however, the model based on a pure CR chondrite composition produced the poorest fit to the NWA 011 composition, with CaO/Al_2O_3 ratios that were far too high. The model was based on the composition of CR chondrite Y-790112, which is the closest match to NWA 011 in terms of oxygen isotopic composition. The CR chondrites are part of a large CR chondrite clan that also includes the CH (high metal) chondrites, the CB (Bencubbin) chondrites and ungrouped LEW 85332 (Weisberg et al. 1995; Krot et al. 2002). Although these meteorite groups are related by a number of characteristics, including oxygen isotopic compositions, there are chemical and mineralogical differences between them. Thus, a different member of this clan may provide a better fit as the source material for NWA 011.

Trace element compositions provide few constraints on the NWA 011 parent, as all the chondrites have unfractionated REE patterns. However, as we noted earlier, NWA 011 is depleted in Mn relative to eucrites, leading to its distinctive Fe/Mn ratio (Fig. 3). The CR chondrite clan meteorites (CR, CB, and CH) are all highly depleted in volatile lithophile elements, including Mn, relative to other chondrites (Weisberg et al. 1995), suggesting a possible link to the NWA 011 parent material. Moreover, some of the CR chondrite clan meteorites are highly enriched in refractory and normal siderophile elements, including the CH and CB chondrite groups (Krot et al. 2002). NWA 011 has high siderophile element abundances with highly fractionated Ni/Ir and Ni/Co ratios. Korotchantseva et al. (2003) suggested that oxidizing conditions in the NWA 011 source may have prevented complete equilibration with Fe metal (accounting for the elevated siderophile element abundances) and noted that the high Fe/Mn and high P contents in NWA 011 support an oxidized source region. Our major element data also provide some evidence for oxidizing conditions from the presence of Fe_2O_3 in ulvöspinel and pyroxene (Table 2). Ulvöspinel from NWA 011 contains 2.3 wt.% of Fe_2O_3, significantly higher than the Fe_2O_3 contents of HED chromites, which are typically less than 1 wt.% (Mittlefehldt 1994; Mittlefehldt et al. 1998).

Origin of NWA 011 on Mercury?

Commenting on the discovery by Yamaguchi et al. (2002) that NWA 011 has an oxygen isotopic composition different from that of the eucrites and therefore must come from a distinct source, Palme (2002) suggested that perhaps NWA 011 is of Mercurian origin. The discovery and identification of a meteorite from Mercury would be of great scientific value and the probability of a Mercurian sample reaching Earth, while low, is not negligible (estimated to be about 1% of that from Mars; Love and Keil [1995]). However, NWA 011 does not appear to be that sample. Love and Keil (1995) noted that Mercurian rocks should probably have low volatile contents and be moderately enriched in refractory lithophile elements. Most Mercurian surface rocks are probably volcanic and should contain <5% FeO. NWA 011, with its very Fe-enriched composition, clearly does not match these expectations. Moreover, the Sm-Nd age of NWA 011 of 4.46 Ga (Nyquist et al. 2003) is older than the estimated solidification ages of ~3.7 to ~4.4 Ga for rocks from Mercury (Love and Keil 1995) and suggests an asteroidal rather than Mercurian origin. The exposure age of NWA 011 is similar to that of eucrites (Yamaguchi et al. 2002; Bogard and Garrison 2004) and, thus, also suggests an asteroidal origin.

The only known basaltic asteroid other than 4 Vesta in the asteroid belt is 1459 Magnya (Lazarro et al. 2000). This small (~30 km) rock has no known dynamical links to 4 Vesta or any other nearby large asteroids, but orbital resonances in the region of the asteroid belt around 1459 Magnya indicate that it could be a rare surviving portion of a larger differentiated body that was disrupted long ago (Lazarro et al. 2000). NWA 011 could be a fragment of this parent body, as also suggested by Nyquist et al. (2003).

CONCLUSIONS

The NWA 011 basalt originated from a source with roughly chondritic proportions of the REE, like the eucrites it was initially identified with. A slightly LREE-enriched bulk composition with a small positive Eu anomaly, as well as highly fractionated Fe/Mg ratios and depleted Sc abundances (Korotchantseva et al. 2003), suggest that the NWA 011 source experienced some pyroxene and/or olivine fractionation. Metamorphism of NWA 011 resulted in homogenization of REE abundances within grains, but this meteorite does not seem to have experienced the intergrain REE redistribution seen in some highly metamorphosed eucrites. Despite a similarity in oxygen isotopic compositions, NWA 011 is probably not genetically related to the acapulcoites and lodranites. The source material for NWA 011 may have been like some CH or CB chondrites, members of

the CR chondrite clan with similar oxygen isotopic compositions. The NWA 011 parent body is probably of asteroidal origin, possibly the basaltic asteroid 1459 Magnya.

Acknowledgments–This work was supported by NASA grants NAG-NNG04GG49G to C. F., NAG5-11558 to L. A. T., and NAG5-12948 to D. R. We thank T. Smolar and E. Inazaki for maintenance of the 3f ion microprobe at Washington University. Careful reviews by A. Ruzicka and K. Righter provided significant improvements to this paper and are much appreciated.

Editorial Handling—Dr. Kevin Righter

REFERENCES

Afanasiev S. V., Ivanova M. A., Korotchantseva E. V., Kononkova N. N., and Nazarov M. A. 2000. Dhofar 007 and Northwest Africa 011: Two new eucrites of different types (abstract). *Meteoritics & Planetary Science* 35:A19.

Alexander C. M. O. 1994. Trace element distributions within ordinary chondrite chondrules: Implications for chondrule formation conditions and precursors. *Geochimica et Cosmochimica Acta* 58:3451–3467.

Anders E. and Grevesse N. 1989. Abundances of the elements: Meteoritic and solar. *Geochimica et Cosmochimica Acta* 53:197–214.

Ash R. D. and Pillinger C. T. 1995. Carbon, nitrogen, and hydrogen in Saharan chondrites: The importance of weathering. *Meteoritics* 30:85–92.

Barrat J. A., Gillet P., Lesourd M., Blichert-Toft J., and Poupeau G. R. 1999. The Tatahouine diogenite: Mineralogical and chemical effects of sixty-three years of terrestrial residence. *Meteoritics & Planetary Science* 34:91–97.

Basaltic Volcanism Study Project. 1981. Basaltic volcanism on the terrestrial planets. New York: Pergamon Press. 1286 pp.

Binzel R. P. and Xu S. 1993. Chips off of asteroid 4 Vesta: Evidence for the parent body of basaltic achondrite meteorites. *Science* 260:186–191.

Bland P. A., Berry F. J., Smith T. B., Skinner S. J., and Pillinger C. T. 1996. The flux of meteorites to the Earth and weathering in hot desert ordinary chondrite finds. *Geochimica et Cosmochimica Acta* 60: 2053–2059.

Boesenberg J. 2003. An oxygen isotope mixing model for the Northwest Africa 011 basaltic achondrite (abstract #1239). 34th Lunar and Planetary Science Conference. CD-ROM.

Bogard D. and Garrison D. 2003. ^{39}Ar-^{40}Ar ages of eucrites and thermal history of asteroid 4 Vesta. *Meteoritics & Planetary Science* 38:669–710.

Bogard D. and Garrison D. 2004. ^{39}Ar-^{40}Ar dating of unusual eucrite NWA 011: Is it from Vesta? (abstract #1094). 35th Lunar and Planetary Science Conference. CD-ROM.

Clayton R. N. 1993. Oxygen isotopes in meteorites. *Annual Reviews in Earth and Planetary Science* 21:115–149.

Clayton R. N. 2003. Oxygen isotopes in meteorites. In *Meteorites, planets and comets*, edited by Davis A. M. Oxford: Elsevier Science. pp. 129–142.

Clayton R. N. and Mayeda T. K. 1996. Oxygen isotope studies of achondrites. *Geochimica et Cosmochimica Acta* 60:1999–2017.

Consolmagno G. J. and Drake M. J. 1977. Composition and evolution of the eucrite parent body: Evidence from rare earth elements. *Geochimica et Cosmochimica Acta* 41:1271–1282.

Crozaz G. and Wadhwa M. 2001. The terrestrial alteration of Saharan shergottites Dar al Gani 476 and 489: A case study of weathering in a hot desert environment. *Geochimica et Cosmochimica Acta* 65:971–978.

Crozaz G., Floss C., and Wadhwa M. 2003. Chemical alteration and REE mobilization in meteorites from hot and cold deserts. *Geochimica et Cosmochimica Acta* 67:4727–4741.

Dreibus G., Huisl W., Haubold R., and Jagoutz E. 2001. Influence of terrestrial desert weathering in martian meteorites (abstract). *Meteoritics & Planetary Science* 36:A50–A51.

Eugster O. and Michel T. 1995. Common asteroid break-up events of eucrites, diogenites, and howardites and cosmic-ray production rates for noble gases in achondrites. *Geochimica et Cosmochimica Acta* 59:177–199.

Floss C. 2000. Complexities on the acapulcoite-lodranite parent body: Evidence from trace element distributions in silicate minerals. *Meteoritics & Planetary Science* 35:1073–1085.

Floss C. and Jolliff B. 1998. Rare earth element sensitivity factors in calcic plagioclase (anorthite). In *Secondary ion mass spectrometry: SIMS XI*, edited by Gillen G., Lareau R., Bennett J., and Stevie F. New York: John Wiley & Sons. pp. 785–788.

Floss C., James O. B., McGee J. J., and Crozaz G. 1998. Lunar ferroan anorthosite petrogenesis: Clues from trace element distributions in FAN subgroups. *Geochimica et Cosmochimica Acta* 62:1255–1283.

Floss C., Crozaz G., Yamaguchi A., and Keil K. 2000. Trace element constraints on the origins of highly metamorphosed Antarctic eucrites. *Antarctic Meteorite Research* 13:222–237.

Floss C., Taylor L. A., and Promprated P. 2004. Trace element systematics of Northwest Africa 011: A "eucritic" basalt from a non-eucrite parent body (abstract #1153). 35th Lunar and Planetary Science Conference. CD-ROM.

Goodrich C. A. and Delaney J. S. 2000. Fe/Mg-Fe/Mn relations of meteorites and primary heterogeneity of primitive achondrite parent bodies. *Geochimica et Cosmochimica Acta* 64:149–160.

Grossman J. N. 2000. The Meteoritical Bulletin no. 84. *Meteoritics & Planetary Science* 35:A199–A225.

Hsu W. 1995. Ion microprobe studies of the petrogenesis of enstatite chondrites and eucrites. Ph.D. thesis, Washington University, St. Louis, Missouri, USA.

Hsu W. and Crozaz G. 1996. Mineral chemistry and the petrogenesis of eucrites: I. Noncumulate eucrites. *Geochimica et Cosmochimica Acta* 60:4571–4591.

Kitts K. and Lodders K. 1998. Survey and evaluation of eucrite bulk compositions. *Meteoritics & Planetary Science* 33:A197–A213.

Korotchantseva E. V., Ivanova M. A., Lorenz C. A., Bouikine A. I., Trieloff M., Nazarov M. A., Promprated P., Anand M., and Taylor L. A. 2003. Major and trace element chemistry and Ar-Ar age of the NWA 011 achondrite (abstract #1575). 34th Lunar and Planetary Science Conference. CD-ROM.

Kretz R. 1982. Transfer and exchange equilibria in a portion of the pyroxene quadrilateral as deduced from natural and experimental data. *Geochimica et Cosmochimica Acta* 46:411–421.

Krot A. N., Meibom A., Weisberg M. K., and Keil K. 2002. The CR chondrite clan: Implications for the early solar system processes. *Meteoritics & Planetary Science* 37:1451–1490.

Jolliff B. L., Haskin L. A., Colson R. O., and Wadhwa M. 1993. Partitioning in REE-saturating minerals: Theory, experiment, and modelling of whitlockite, apatite, and evolution of lunar residual magmas. *Geochimica et Cosmochimica Acta* 57:4069–4094.

Jones J. H. 1995. Experimental trace element partitioning. In *Rock physics and phase relations, a handbook of physical constants*, edited by Ahrens T. J. Washington, D. C.: American Geophysical Union. pp. 73–104.

Lazzaro D., Michtchenko T., Carvano J. M., Binzel R. P., Bus S. J., Burbine T. H., Mothe-Diniz T., Florczak M., Angeli C. A., and Harris A. W. 2000. Discovery of a basaltic asteroid in the outer main belt. *Science* 288:2033–2035.

Love S. G. and Keil K. 1995. Recognizing mercurian meteorites. *Meteoritics* 30:269–278.

McCord T. B., Adams J. B., and Johnson T. V. 1970. Asteroid Vesta: Spectral reflectivity and compositional implications. *Science* 168:1445–1447.

McCoy T. J., Keil K., Clayton R. N., Mayeda T. K., Bogard D. D., Garrison D. H., Huss G. R., Hutcheon I. D., and Wieler R. 1996. A petrologic, chemical, and isotopic study of Monument Draw and comparison with other acapulcoites: Evidence for formation by incipient partial melting. *Geochimica et Cosmochimica Acta* 60:2681–2708.

McCoy T. J., Keil K., Clayton R. N., Mayeda T. K., Bogard D. D., Garrison D. H., and Wieler R. 1997a. A petrologic and isotopic study of lodranites: Evidence for early formation as partial melt residues from heterogeneous precursors. *Geochimica et Cosmochimica Acta* 61:623–637.

McCoy T. J., Keil K., Muenow D. W., and Wilson L. 1997b. Partial melting and melt migration in the acapulcoite-lodranite parent body. *Geochimica et Cosmochimica Acta* 61:639–650.

McKay G., Wagstaff J., and Yang S. R. 1986. Clinopyroxene REE distribution coefficients for shergottites: The REE content of the Shergotty melt. *Geochimica et Cosmochimica Acta* 50:927–937.

Miller M. F. 2002. Isotopic fractionation and the quantification of ^{17}O anomalies in the oxygen three-isotope system: An appraisal and geochemical significance. *Geochimica et Cosmochimica Acta* 66:1881–1889.

Mittlefehldt D. W. 1994. ALH 84001, a cumulate orthopyroxenite member of the martian meteorite clan. *Meteoritics* 29:214–221.

Mittlefehldt D. W. and Lindstrom M. M. 1991. Generation of abnormal trace element abundances in Antarctic eucrites by weathering processes. *Geochimica et Cosmochimica Acta* 55: 77–87.

Mittlefehldt D. W., Lindstrom M. M., Bogard D. D., Garrison D. H., and Field S. W. 1996. Acapulco- and lodran-like achondrites: Petrology, geochemistry, chronology, and origin. *Geochimica et Cosmochimica Acta* 60:867–882.

Mittlefehldt D. W., McCoy T. J., Goodrich C. A., and Kracher A. 1998. Non-chondritic meteorites from asteroidal bodies. In *Planetary materials*, edited by Papike J. J. Washington, D. C.: Mineralogical Society of America. 195 p.

Nyquist L., Shih C.-Y., Wiesman H., Yamaguchi A., and Misawa K. 2003. Early volcanism on the NWA 011 parent body (abstract). *Meteoritics & Planetary Science* 38:A59.

Palme H. 2002. A new solar system basalt. *Science* 296:271–273.

Papike J. J. 1998. Comparative planetary melt-derived mineralogy. In *Planetary materials*, edited by Papike J. J. Washington, D. C.: Mineralogical Society of America. 11 p.

Patzer A., Hill D. H., and Boynton W. V. 2004. Evolution and classification of acapulcoites and lodranites from a chemical point of view. *Meteoritics & Planetary Science* 39:61–85.

Promprated P., Taylor L. A., Anand M., Rumble D., Korotchantseva E. V., Ivanova M. A., Lorenz C. A., and Nazarov M. A. 2003. Petrology and oxygen isotopic compositions of anomalous achondrite NWA 011 (abstract #1757). 34th Lunar and Planetary Science Conference. CD-ROM.

Schreiber H. D., Lauer H. V. Jr., and Thanyasiri T. 1980. The redox state of cerium in basaltic magmas: An experimental study of iron-cerium interactions in silicate melts. *Geochimica et Cosmochimica Acta* 44:1599–1612.

Scott E. R. D. 1979. Origin of iron meteorites. In *Asteroids*, edited by Gehrels T. Tucson, Arizona: The University of Arizona Press. pp. 892–925.

Scherer P., Schultz L., and Loeken T. 1994. Weathering and atmospheric noble gases in chondrites. In *Noble gas geochemistry and cosmochemistry*, edited by Matsuda J. Tokyo: Terra Scientific Publishing Co. pp. 43–53.

Sharp Z. D. 1990. A laser-based microanalytical method for the in situ determination of oxygen isotope ratios of silicates and oxides. *Geochimica et Cosmochimica Acta* 54:1353–1357.

Spear F. S. 1995. Metamorphic phase equilibria and pressure-temperature-time paths. Washington, D. C.: Mineralogical Society of America. 799 pp.

Swindle T. D., Kring D. A., Burkland M. K., Hill D. H., and Boynton W. V. 1998. Noble gases, bulk chemistry, and petrography of olivine-rich achondrites Eagles Nest and Lewis Cliff 88763: Comparison to brachinites. *Meteoritics & Planetary Science* 33: 31–48.

Takeda H. and Graham A. L. 1991. Degree of equilibration of eucritic pyroxenes and thermal metamorphism of the earliest planetary crust. *Meteoritics* 26:129–134.

Valley J. W., Kitchen N. E., Kohn M. J., Niendorf C. R., and Spicuzza M. J. 1995. UWG-2, a garnet standard for oxygen isotope ratios: Strategies for high precision and accuracy with laser heating. *Geochimica et Cosmochimica Acta* 59:5223–5231.

Wakefield K., Bogard D., and Garrison D. 2004. Cosmic ray exposure ages, Ar-Ar ages, and the origin and history of eucrites (abstract #1020). 35th Lunar and Planetary Science Conference. CD-ROM.

Warren P. H. and Jerde E. A. 1987. Composition and origin of Nuevo Laredo trend eucrites. *Geochimica et Cosmochimica Acta* 51: 713–725.

Weisberg M., Prinz M., Clayton R., and Mayeda T. K. 1993. The CR (Renazzo-type) carbonaceous chondrite group and its implications. *Geochimica et Cosmochimica Acta* 57:1567–1586.

Weisberg M., Prinz M., Clayton R., Mayeda T. K., Grady M. M., and Pillinger C. T. 1995. The CR chondrite clan. *Proceedings of the NIPR Symposium on Antarctic Meteorites* 8:11–32.

Wiechert U., Halliday A. N., Lee D.-C., Snyder G., Taylor L. A., and Rumble D. 2001. Oxygen isotopes and the moon-forming giant impact. *Science* 294:345–348.

Wiechert U., Halliday A. N., Palme H., and Rumble D. 2002. Oxygen isotopic heterogeneity among eucrites (abstract). *Geochimica et Cosmochimica Acta* 66:A834.

Yamaguchi A. 2001. Mineralogical study of a highly metamorphosed eucrite, Northwest Africa 011 (abstract #1578). 32nd Lunar and Planetary Science Conference. CD-ROM.

Yamaguchi A., Taylor G. J., Keil K., Floss C., Crozaz G., Nyquist L. E., Bogard D. D., Garrison D., Reese Y., Wiesman H., and Shih C.-Y. 2001. Post-crystallization reheating and partial melting of eucrite EET 90020 by impact into the hot crust of 4 Vesta ~4.50 Ga ago. *Geochimica et Cosmochimica Acta* 65:3577–3599.

Yamaguchi A., Clayton R. N., Mayeda T. K., Ebihara M., Oura Y., Miura Y. N., Haramura H., Misawa K., Kojima H., and Nagao K. 2002. A new source of basaltic meteorites inferred from Northwest Africa 011. *Science* 296:334–336.

Zinner E. and Crozaz G. 1986a. A method for the quantitative measurement of rare earth elements by ion microprobe. *International Journal of Mass Spectrometry and Ion Processes* 69:17–38.

Zinner E. and Crozaz G. 1986b. Ion probe determination of the abundances of all the rare earth elements in single mineral grains. In *Secondary ion mass spectrometry, SIMS V*, edited by Benninghoven A., Colton R. J., Simons D. S., and Werner H. W. New York: Springer-Verlag. pp. 444–446.